Preprints of the 19th World Congress
The International Federation of Automatic Control
Cape Town, South Africa. August 24-29, 2014

Limits of Observability in Large-Scale Linear Networked Clocks ⋆

Elma O'Sullivan-Greene * **Iven Mareels** *

* *Department of Electrical and Electronic Engineering, The University of Melbourne, Victoria, Australia (e-mail:elmaog@unimelb.edu.au)*

Abstract: Large-scale networks of undamped coupled oscillators represent both modern engineered systems and systems from the biological world. The neural network of the brain is a particular example of motivating interest. The degree to which tracking, predicting and controlling dynamics in such networks will be successful is conditional on observability. Observability is considered using large-scale networked clocks, a linearisation of networked oscillators, through the structure of the observability matrix using Vandermonde matrices. Observability is found to be particularly poor for these undamped networked clocks. This raises interesting challenges to elucidate sufficient information from these networks for therapeutic benefit in medical bionics.

Keywords: Network Observability, Biomedical Systems, Neural Dynamics, Brain Models, Large-scale Systems

1. INTRODUCTION

Coupled oscillators networks are fascinating both in the phenomenon they exhibit and in the diversity of real-world examples they model. Phenomenon include self-synchronisation, that is the ability of coupled oscillators to merge into collective behaviour without the need for a conductor or driving node in the network. Coupled oscillator networks can model many engineered distributed systems that exhibit self-organising behaviour through synchronisation from modern telecommunications (Prehofer and Bettstetter (2005)) to future power systems (Butler (2007); Rohden et al. (2012)). The natural world is also replete with examples, from synchronously flashing fireflies to the neural networks of brain tissue (Strogatz and Stewart (1993)).

Observability of these oscillatory networks has motivations in the need to extract information from such systems, both human-engineered and biological, to predict, track and control their dynamics. Networked clocks, as investigated in this paper, are the linearised counterpart to networks of coupled non-linear oscillators. An initial insight into oscillator network observability is considered using linear approaches.

Existing work in network observability, from early work in Wu and Monticelli (1985) and Monticelli and Wu (1985) to more recent advancements in Liu et al. (2013), seeks to exploit redundancies in connection pathways so that all states are reachable, through network pathways, from a subset of states that directly influence the the system output. By contrast, in this paper we explore a network with fully connected graph. There is an absence of any connection redundancies by construction, since each state is connected through network pathways to every other state. This provides a network that is theoretically observable by measuring from a single state (any single state), however, severe practical challenges to observability are found for these networks.

This paper presents a coupled oscillator model in Section 2. A structural analysis of the observability matrix for the network using Vandermonde matrices is considered analytically, under the extreme condition of maximally separated clock frequencies, in Section 3. An analysis of the broader range of possible observability outcomes, for clock frequencies drawn from (*i*) a uniform distribution and (*ii*) a Gaussian distribution, is provided through simulation in Section 4, followed by conclusions in Section 5.

2. NETWORK CLOCK MODEL

Inspired by the neural networks of the brain, we use a generic and scalable network clock model based on coupled second order pendula. Wright et al. (1985) devised a similar coupled oscillator model in 1985 to model state changes in brain activity as measured by EEG (Electroencephalography), that is, electrical recordings from the brain. Further background on EEG recordings can be found in Ch. 2 of Varsavsky et al. (2010) and in Niedermeyer and Lopes Da Silva (2005). As a generic synthetic model which neglects the complexities of biologically realistic neuron-dynamics, this is not a model which can tell us anything about the nature of brain function. This approach is rather suited instead to the specific task of investigating what underlying information one may expect to recover from an observation comprised of a linear map of the state. Variations of this model were also used towards preliminary analysis on the brain observation problem (O'Sullivan-Greene et al. (2009a,b); OSullivan-Greene et al. (2011)).

Each individual oscillator is modelled as a linearised undamped pendulum clock,

⋆ This research was supported by The University of Melbourne's Early Career Academic Fellowship Scheme.

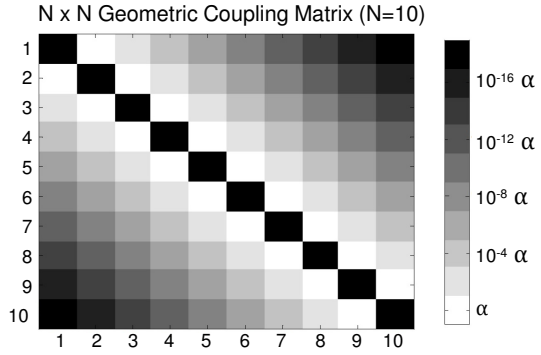

Fig. 1. An image showing the structure of the coupling matrix for a 2-D network of $N = 10$ clocks with a fully connected graph. The white boxes indicate that each clock is coupled to its nearest neighbours with the maximum coupling magnitude of α. Coupling strength to other clocks is geometrically decaying by distance of clock i to clock j as indicated by the accompanying greyscale bar. The black boxes indicate that each clock is not coupled to itself.

$$\ddot{x}_i + \tilde{\omega}_i^2 x_i = F_i, \ i = 1 \dots N, \tag{1}$$

where x_i is the angular position, $\tilde{\omega}_i$ is the natural frequency of oscillation and F_i is the forcing term of the i^{th} pendulum defined in (2).

$$F_i = \sum_j \alpha_{ij}(x_j - x_i), \tag{2}$$

F_i consists of a feedback term that couples the position state from other pendula, $\sum_j \alpha_{ij}(x_j - x_i)$. α_{ij} denotes the coupling strength between clocks i and j.

A simple fully-connected graph is assumed, with strong local connection and weaker long range connection, as illustrated in Fig. 1. Additionally, it is assumed that all model parameters are known.

It is chosen to restrict the model to pure or marginally stable oscillators rather than include a damping term. While certainly the brain will naturally deviate into both slightly underdamped and slightly damped modes of oscillation, it is envisioned that the natural balance of excitability in the brain will constrain this damped and underdamped activity to dynamics that lie near to the critically damped boundary.

A coupled clock network of N linear clocks (illustrated for $N = 4$ in Fig. 2) can be written in state space format as $\dot{\mathbf{x}} = \mathbf{A}\mathbf{x}$ with an ideal EEG measurement of $\mathbf{y} = \mathbf{C}\mathbf{x}$ using $(\mathbf{A}, \mathbf{C})$ defined in (3,7) where $\mathbf{x}$ is the state.

$$\mathbf{A} = \begin{bmatrix} \mathbf{A}_1 + \varepsilon_{11} & \varepsilon_{12} & \dots & \varepsilon_{1N} \\ \varepsilon_{21} & \mathbf{A}_2 + \varepsilon_{22} & \dots & \varepsilon_{2N} \\ \vdots & \vdots & \ddots & \vdots \\ \varepsilon_{N1} & \varepsilon_{N2} & \dots & \mathbf{A}_N + \varepsilon_{NN} \end{bmatrix}, \tag{3}$$

where

$$\mathbf{A}_i = \begin{pmatrix} 0 & -\tilde{\omega}_i \\ +\tilde{\omega}_i & 0 \end{pmatrix}, \tag{4}$$

$$\varepsilon_{ij} = \begin{pmatrix} 0 & 0 \\ -\alpha_{ij} & 0 \end{pmatrix} \text{for i} \neq \text{j}, \tag{5}$$

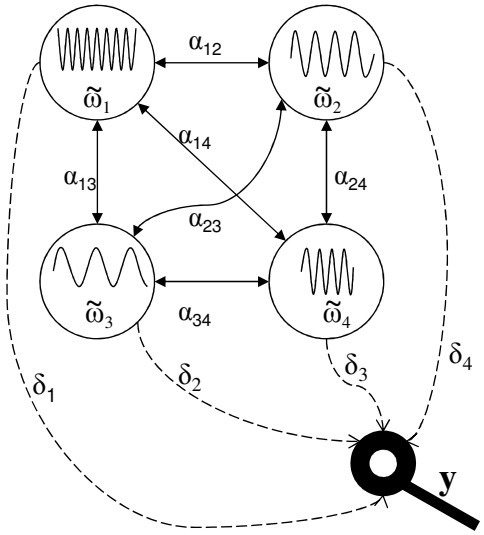

Fig. 2. A network of four interconnecting clocks. Each clock has an oscillation frequency $\tilde{\omega}_i$. The coupling between clocks i and j is given by α_{ij}, and a measurement electrode connects to each clock with strength δ_i.

$$\varepsilon_{ii} = \begin{pmatrix} 0 & 0 \\ +\sum_{k=1}^{N} \alpha_{ik} & 0 \end{pmatrix}, \tag{6}$$

$$\mathbf{C} = [\, 0 \ \delta_1 \ 0 \ \delta_2 \cdots \ 0 \ \delta_N \,], \tag{7}$$

where δ_i indicates the relative importance of clock i in the EEG output signal (the entries of the measurement vector $\mathbf{C}$ satisfy $\delta_i \geq 0$ and $\sum_i \delta_i = 1$). Coupling is chosen to be symmetric ($\alpha_{ij} = \alpha_{ji}$) and positive ($\alpha_{ij} > 0 \ \forall \ i, j$).

For this coupling configuration it is assumed that the clocks are spatially organised along a 1-dimensional structure (see Figure 3). Other spatial constructs, such as extending to 2 or 3 dimensions, would also be possible for alternative connectivity coefficients.

Consider now the discrete formulation of the system model given in (9, 10), using the mapping,

$$\mathbf{A} \to e^{\mathbf{A}\Delta T} = \widetilde{\mathbf{A}}. \tag{8}$$

For simplicity and generic problem formulation we use a normalised sampling time $\Delta T = 1$ and normalised frequency range $\tilde{\omega}_i \in (0, 1]$.

$$\mathbf{x}_{k+1} = \widetilde{\mathbf{A}}\mathbf{x}_k \tag{9}$$
$$\mathbf{y}_k = \mathbf{C}\mathbf{x}_k \tag{10}$$

The discrete version of the system in (9) is convenient for the analysis undertaken in Section 3 and the discrete measurement in (10) is appropriate since all real measurements are digital in nature.

Next the model presented here will be used to explore the question of: *How observable is* $\mathbf{x} \in \boldsymbol{R}^N$ *given* $\mathbf{y} \in \boldsymbol{R}^M$*?* Of particular interest, given the motivational problem of observing the brain state from EEG measurements, is when system order N is particularly large compared to

the number of measurements M (with one state assigned per neuron $N \approx 10^{11}$, while typically $M < 30$).

3. STRUCTURE OF THE OBSERVABILITY MATRIX

The observability matrix, $\mathcal{O}(\mathbf{C}, \widetilde{\mathbf{A}})$, can be deconstructed using Vandermonde matrices to gain an insight into the expected observability properties as a function of network size. See (Golub and Van Loan, 2013, Ch. 4) for background information on Vandermonde matrices.

Since $\widetilde{\mathbf{A}}$ (8) contains eigenvalues on the unit circle [1], $\widetilde{\mathbf{A}}$ can be generically diagonalised to,

$$\mathbf{T}^{-1}\widetilde{\mathbf{A}}\mathbf{T} = diag([e^{j\omega_1}, e^{-j\omega_1}, ..., e^{j\omega_N}, e^{-j\omega_N}]). \quad (11)$$

The diagonalising state transformation, $\mathbf{T}$, also converts the $\mathbf{C} = [0, \delta_1, 0, \delta_2, \ldots]$ given in (7) to the full vector, $\mathbf{CT} = [\delta_1, \delta_1, \delta_2, \delta_2, \ldots]$. If $\delta_i = 1 \ \forall \ i$, $\mathcal{O}(\mathbf{CT}, \mathbf{T}^{-1}\widetilde{\mathbf{A}}\mathbf{T})$ is a Vandermonde matrix, $\mathbf{V}$,

$$\mathbf{V} = \begin{bmatrix} 1 & 1 & 1 & \cdots & 1 \\ e^{j\omega_1} & e^{-j\omega_1} & e^{j\omega_2} & \cdots & e^{-j\omega_N} \\ e^{j2\omega_1} & e^{-j2\omega_1} & e^{j2\omega_2} & \cdots & e^{-j2\omega_N} \\ \vdots & \vdots & \vdots & \ddots & \vdots \\ e^{j(2N-1)\omega_1} & e^{-j(2N-1)\omega_1} & e^{j(2N-1)\omega_2} & \cdots & e^{-(2N-1)j\omega_N} \end{bmatrix}, \quad (12)$$

Then for a $\mathbf{C}$ vector containing any δ_i, $\mathcal{O}(\mathbf{CT}, \mathbf{T}^{-1}\widetilde{\mathbf{A}}\mathbf{T}) = diag(\mathbf{CT})\mathbf{V}$. The determinant of the observability matrix is:

$$\begin{aligned} &det\left(\mathcal{O}\left(\mathbf{CT}, \mathbf{T}^{-1}\widetilde{\mathbf{A}}\mathbf{T}\right)\right) \\ &\quad = det\left(diag(\mathbf{CT})\right) det\left(\mathbf{V}\right) \\ &\quad = \underbrace{\prod_{i=1}^{N}(\delta_i)^2}_{Channel\ Model} \underbrace{\prod_{1\le i<j\le(2N-1)} (e^{j\gamma_j} - e^{j\gamma_i})}_{Network\ Model} \end{aligned} \quad (13)$$

where

$$\begin{cases} \gamma_{2i-1} = \omega_i \\ \gamma_{2i} = -\omega_i. \end{cases} \quad (14)$$

(13) is factorised into two distinct components, a channel model and a network model. The network model gives us the intrinsic information content in the network. The channel model provides the read-out of information content from the network.

Consider next the case where (13) is maximised. The most well-connected channel model provides the maximum read-out available. Since δ_i is constrained by $\sum_i \delta_i = 1, \delta_i > 0$ then a uniform measure of the state where $\delta_i = \frac{1}{N} \ \forall \ i$ gives the maximum read out of information content. A maximally informative oscillator network (providing the most energy in the determinant) would have eigenvalues uniformly separated around the unit circle (intuitively, multiple well-separated frequencies are easier to observe than a dense spectral arrangement with same number of frequencies). Next the determinant of the Vandermonde Matrix is evaluated for this case of eigenvalues of $\widetilde{\mathbf{A}}$ uniformly distributed around the unit circle ($\omega_i = \frac{k\pi}{2N}$, for $i = 1, 2, \ldots, N,$ and $k = 2i - 1$).

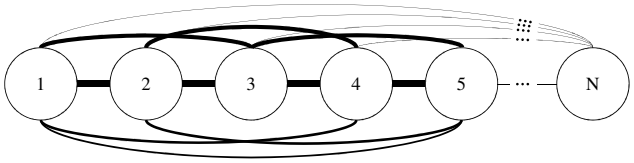

Fig. 3. The spatial organisation for a 1-dimensional network of N clocks. Each circle represents a clock and the connection line thickness depicts the strength of connection.

Theorem 1. For the Vandermonde matrix $\mathbf{V}$ in (12) that represents a coupled oscillator network model,

$$det(\mathbf{V}) = j^N N^N 2^N, \quad (15)$$

under the condition that the network's eigenvalues are chosen to be maximally separated around the unit circle.

Proof. From (13) we have that:

$$det(\mathbf{V}) = \prod_{1\le i<j\le(2N-1)} (e^{j\gamma_j} - e^{j\gamma_i}), \quad (16)$$

This can be expanded, as shown in (18), using $\gamma_{2i-1} = \omega_i$, $\gamma_{2i} = -\omega_i$ and (17).

$$\omega_i = \frac{k\pi}{2N}, \text{ for } i = 1, 2, \ldots, N, \text{ and } k = 2i - 1. \quad (17)$$

These frequencies, ω_i, are chosen such that $e^{j\gamma_i}$ are uniformly distributed around the unit circle for maximum separation between eigenvalues.

$$\begin{aligned} det(\mathbf{V}) =& (e^{-j\omega_1} - e^{j\omega_1})(e^{j\omega_2} - e^{-j\omega_1}) \\ &.(e^{j\omega_2} - e^{j\omega_1})(e^{-j\omega_2} - e^{j\omega_2}) \\ &.(e^{-j\omega_2} - e^{-j\omega_1})(e^{-j\omega_2} - e^{j\omega_1}) \ldots \\ =& \overbrace{(2j\sin(\omega_1))\,(2j\sin(\omega_2)) \ldots}^{\text{Euler pairs}} \\ &\underbrace{.\left(4\left(2\sin\left(\tfrac{\omega_1+\omega_2}{2}\right)\sin\left(\tfrac{\omega_1-\omega_2}{2}\right)\right)^2\right)\ldots}_{\text{Remaining exponential pairs}} \end{aligned} \quad (18)$$

There are N Euler pair terms and $\frac{N!}{2!(N-2)!} = \frac{N(N-1)}{2}$ remaining exponential pairs terms for combinations of (ω_i, ω_j).

[1] The clock network can be written in continuous form as, $\ddot{\mathbf{x}} + \mathbf{W}\mathbf{x} = 0$ where $\ddot{\mathbf{x}} = [\ddot{x}_1 \ \ddot{x}_2 \ \ldots \ \ddot{x}_N]'$, $\mathbf{x} = [x_1 \ x_2 \ \ldots \ x_N]'$ ($'$ denotes transpose) and

$$\mathbf{W} = \begin{pmatrix} \tilde{\omega}_1^2 + \sum_j \alpha_{1j} & -\alpha_{12} & -\alpha_{13} & \cdots & -\alpha_{1N} \\ -\alpha_{12} & \tilde{\omega}_2^2 + \sum_j \alpha_{2j} & -\alpha_{23} & \cdots & -\alpha_{2N} \\ -\alpha_{13} & -\alpha_{23} & \tilde{\omega}_3^2 + \sum_j \alpha_{3j} & \cdots & -\alpha_{3N} \\ \vdots & \vdots & \vdots & \ddots & \vdots \\ -\alpha_{1N} & -\alpha_{2N} & -\alpha_{3N} & \cdots & \tilde{\omega}_N^2 + \sum_j \alpha_{Nj} \end{pmatrix}$$

$\mathbf{W}$ is a positive definite matrix for $\alpha_{ij} > 0 \ \forall \ i, j$, therefore, there exists $\mathbf{z} = \mathbf{T}\mathbf{x}$ and $\ddot{\mathbf{z}} = \mathbf{D}\mathbf{z}$ such that $\mathbf{D} = \mathbf{T}\mathbf{W}\mathbf{T}^{-1}$ is a diagonal matrix. Specifically, $\mathbf{D} = diag(\omega_1^2, \omega_2^2, \ldots, \omega_N^2)$, where ω_i are the natural frequencies of a purely oscillatory coupled network (a network with $\alpha_{ij} = 0 \ \forall \ i, j$), which are simply shifted or perturbed in frequency from the individual clock natural frequencies $\tilde{\omega}_i$.

$$det(\mathbf{V}) = j^N 2^{2N^2-N} \overbrace{\prod_{i=1}^{N} \sin(\omega_i)}^{\text{Factor a}} \cdot \underbrace{\prod_{(i,j):i<j} \left(\sin\left(\tfrac{\omega_i+\omega_j}{2}\right)\sin\left(\tfrac{\omega_i-\omega_j}{2}\right)\right)^2}_{\text{Factor b}}, \quad (19)$$

Consider the following identity on the geometry of the sine function from Bibak et al. (2009),

$$\prod_{k=1}^{N-1} \sin(\tfrac{k\pi}{N}) = \frac{N}{2^{N-1}}. \quad (20)$$

As a corollary of this,

$$\prod_{k=1}^{N/2} \sin(\tfrac{k\pi}{N}) = \sqrt{\frac{N}{2^{N-1}}}. \quad (21)$$

Using (20), factor a in (19) can be reduced to,

$$\prod_{i=1}^{N} \sin(\omega_i) = \frac{\prod_{k=1}^{2N-1} \sin(\frac{k\pi}{2N})}{\prod_{k=1}^{N-1} \sin(\frac{k\pi}{N})} = \frac{\frac{2N}{2^{2N-1}}}{\frac{N}{2^{N-1}}} = \frac{1}{2^{N-1}}. \quad (22)$$

Due to the geometry of maximally separated eigenvalues around the unit circle, as defined in (17), factor b in (19) can be expressed as,

$$\prod_{i,j:i<j} \left(\sin\left(\tfrac{\omega_i+\omega_j}{2}\right)\sin\left(\tfrac{\omega_i-\omega_j}{2}\right)\right)^2 = \left[\left(\prod_{k=1}^{N} \sin\left(\tfrac{k\pi}{2N}\right)\right)^{N-1} \left(\prod_{k=1}^{N/2} \sin\left(\tfrac{k\pi}{N}\right)\right)\right]^2. \quad (23)$$

Using the identity in (21), (23) becomes,

$$\left[\left(\prod_{k=1}^{N} \sin\left(\tfrac{k\pi}{2N}\right)\right)^{N-1} \left(\prod_{k=1}^{N/2} \sin\left(\tfrac{k\pi}{N}\right)\right)\right]^2 = \left[\left(\sqrt{2N/2^{2N-1}}\right)^{N-1} \left(\sqrt{N/2^{N-1}}\right)\right]^2 = 2^{N-1}\left(\frac{2N}{2^{2N-1}}\right)^N. \quad (24)$$

Substituting (22) and (24) into (19) gives,

$$det(\mathbf{V}) = j^N 2^{2N^2-N} \frac{1}{2^{N-1}} 2^{N-1} \left(\frac{2N}{2^{2N-1}}\right)^N = j^N N^N 2^N. \quad (25)$$

Making the trivial assumption that N is even, gives,

$$det(\mathbf{V}) = N^N 2^N, \quad (26)$$

which completes the proof. □

Corollary 1. As a corollary to Theorem 1, for the observability matrix, $\mathcal{O}\left(\mathbf{C}, \widetilde{\mathbf{A}}\right)$, with $\widetilde{\mathbf{A}}$ defined in (8) and $\mathbf{C}$ defined in (7),

$$det\left(\mathcal{O}\left(\mathbf{C}, \widetilde{\mathbf{A}}\right)\right) = \frac{1}{N^N}, \quad (27)$$

under the condition that the network's eigenvalues are chosen to be maximally separated around the unit circle and there is a uniform measurement of the state.

Proof. From (13) we have that

$$det\left(\mathcal{O}\left(\mathbf{CT}, \mathbf{T}^{-1}\widetilde{\mathbf{A}}\mathbf{T}\right)\right) = \prod_{i=1}^{N} (\delta_i)^2 det(\mathbf{V}), \quad (28)$$

For a uniform measurement of the state $\delta_i = \frac{1}{N} \ \forall \ i$ and (28) becomes,

$$det\left(\mathcal{O}\left(\mathbf{CT}, \mathbf{T}^{-1}\widetilde{\mathbf{A}}\mathbf{T}\right)\right) = \prod_{i=1}^{N} \left(\frac{1}{N}\right)^2 det(\mathbf{V}), \quad (29)$$

Lastly the effect of the transformation $\mathbf{T}$ in (11) should be considered.

$$\mathcal{O}\left(\mathbf{C}, \widetilde{\mathbf{A}}\right) = \mathcal{O}\left(\mathbf{CT}, \mathbf{T}^{-1}\widetilde{\mathbf{A}}\mathbf{T}\right)\mathbf{T}^{-1} \quad (30)$$

where $\mathbf{T}$ is a block diagonal matrix with each diagonal 2×2 block: $[(-j,1)', (+j,1)']$. Using (29), (30) and the results of Theorem 1 gives,

$$det\left(\mathcal{O}(\mathbf{C}, \widetilde{\mathbf{A}})\right) = \underbrace{\prod_{i=1}^{N} \left(\frac{1}{N}\right)^2}_{\frac{1}{N^{2N}}} \underbrace{det(\mathbf{V})}_{j^N N^N 2^N} \underbrace{det(\mathbf{T}^{-1})}_{\left(\frac{-1}{2j}\right)^N} = \frac{(-1)^N}{N^N}, \quad (31)$$

Making the trivial assumption that N is even gives,

$$det\left(\mathcal{O}(\mathbf{C}, \widetilde{\mathbf{A}})\right) = \frac{1}{N^N}, \quad (32)$$

which completes the proof. □

$det\left(\mathcal{O}(\mathbf{C}, \widetilde{\mathbf{A}})\right)$ thus converges to zero with increasing network order N, with a rate that is faster than exponential, despite a very large determinant from the network model alone. This indicates that observability from oscillatory networks is exceedingly ill-posed. That said, however, from a purely numerical representation viewpoint, the very large determinant from the network model is problematic in and of itself. $\mathbf{V}$ comprises of $(2N)^2$ numerically-orderly elements of order 1. Yet $det(\mathbf{V})$ is exceptionally large ($det(\mathbf{V}) \to 2^N N^N$). Exceptionally large determinants are equally as problematic as exceptionally small determinants (for example $det\left(\mathcal{O}(\mathbf{C}, \widetilde{\mathbf{A}})\right) \to \frac{1}{N^N}$) in terms of numerical representation.

4. SIMULATION RESULTS

In the previous section it was found through Theorem 1 that, under the extreme case of maximally separated eigenvalues, the determinant of the Vandermonde matrix that represents the clock network, $det(\mathbf{V})$, grows exponentially with network order N. In this section, through simulation over a range of networks sizes, the range of expected values for $det(\mathbf{V})$ (defined in (16)) is explored more generally by considering (i) eigenspectra uniformly

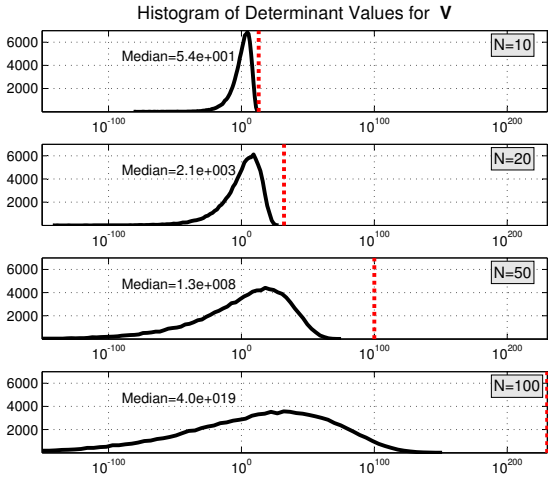

Fig. 4. Histograms of values for determinant of $\mathbf{V}$ for networks of N clocks, where clock network frequencies were drawn from a uniform distribution in the range (0 - π rad/s) over 100,000 trials. Determinant values were distributed across 100 logarithmically spaced bins. The vertical dotted line (in red) is the theoretical limit for maximally spaced frequencies as shown analytically in Theorem 1.

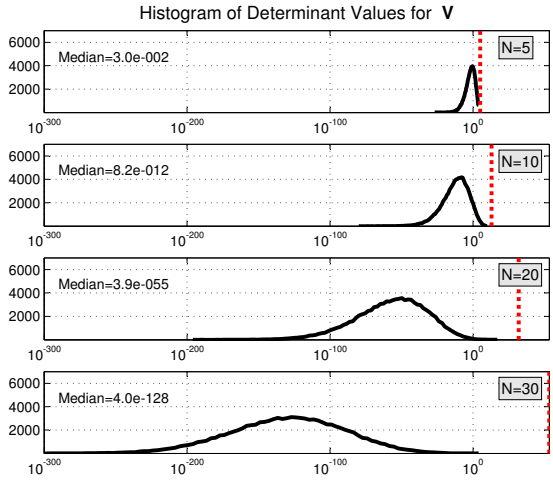

Fig. 5. Histograms of values for determinant of $\mathbf{V}$ for networks of N clocks, where clock network frequencies were drawn from a Gaussian distribution, with mean, $\mu = \frac{\pi}{2}$ and variance $\sigma^2 = 0.5$ over 100,000 trials. Determinant values were distributed across 100 logarithmically spaced bins. The vertical dotted line (in red) is the theoretical limit for equally spaced frequencies as shown analytically in Theorem 1.

distributed around the unit circle and (*ii*) eigenspectra with a truncated Gaussian distribution centred with mean $\mu = \frac{\pi}{2}$ and variance $\sigma^2 = 0.5$ on the unit circle.

4.1 Uniform Distribution

Figure 4 illustrates the range of determinant values for networks where clock network frequencies were drawn from a uniform distribution in the range (0 - π rad/s) over 100,000 trials. This choice of frequencies generates eigenspectra that are uniformly distributed around the unit circle. The absolute values of the resulting determinant values ($|det(\mathbf{V})|$) were distributed across 100 logarithmically spaced bins. The vertical dotted line (in red) is the theoretical limit for equally spaced frequencies as shown analytically in Theorem 1 ($det(\mathbf{V}) = 2^N N^N$, where N is the number of clocks in the network).

The range of possible determinant values is exceptionally broad, from very small values to very large values. This range broadens as N increases. The median value of $|det(\mathbf{V})|$ grows as N increases, however, the gap between the maximum determinant found through simulation and the theoretical $2^N N^N$ limit also increases with N. This is as expected since the likelihood of randomly obtaining N equally separated or near equally separated eigenvalues is low for large N. It is more likely instead that at least some of the eigenvalues will be separated by angles that are significantly smaller than perfectly uniform separation, thus lowering the determinant (since $\sin(\omega_i - \omega_j)$ factors creates small numbers in the overall product in (18) for small $\Delta = \omega_i - \omega_j$.)

4.2 Gaussian Distribution

Biologically, the likelihood of brain networks with uniformly distributed spectral content as described in Section (4) is low. An alternative distribution is therefore explored here. A Gaussian distribution of frequency values is more bio-realistic in the case of the brain's oscillators, where similar frequencies manifest around typical functional behaviour (for example slower oscillations appear during sleep and the auditory cortex oscillates with frequencies to match external auditory stimuli).

Figure 5 illustrates the range of determinant values for networks where clock network frequencies were drawn from a truncated Gaussian distribution with range (0, π), with mean, $\mu = \frac{\pi}{2}$ and variance $\sigma^2 = 0.5$ over 100,000 trials. This choice of frequencies generates eigenspectra that are normally distributed on the unit circle, centred at $\frac{\pi}{2}$. The absolute values of the resulting determinant values were distributed across 100 logarithmically spaced bins. The vertical dotted line (in red) is the theoretical limit for equally spaced frequencies as shown analytically in Theorem 1 ($det(\mathbf{V}) = 2^N N^N$).

Under this Gaussian configuration, the determinant values are all small (predominantly < 1, for $N > 10$). Similar to the case of uniform frequency allocation, the range broadens as N increases and the gap between the maximum determinant found through simulation and the theoretical $2^N N^N$ limit also increases with N. Unlike the uniform case, however, here the median value of $|det(\mathbf{V})|$ decreases as N increases and there exists markedly larger gaps between the determinant values found through simulation and the theoretical $2^N N^N$ limit even for relatively small network sizes of $N = 30$ clocks.

These small determinants and their large distance from the theoretical $2^N N^N$ limit can be explained by the high likelihood of obtaining very small differences between angles with a Gaussian distribution (since $\sin(\omega_i - \omega_j)$

factors creates exceptionally small numbers in the overall product in (18) for $\Delta = \omega_i - \omega_j \approx 0$.)

5. CONCLUSIONS

Using a highly abstracted model of a coupled oscillator brain network, practical observability of such systems is found to be exceptionally poor. This abstracted problem formulation is a simplification of any real world problem with all parameters known and by dealing with a stationary environment. These systems are theoretically observable. The pair $(\mathbf{C}, \mathbf{A})$ of form given in (7) and (3) can be shown to be observable using the Popov-Belevitch-Hautus test (Kailath, 1980, Ch 2), even in the case where only a single state is connected to the output ($\delta_i = 0 \; \forall \; i \neq k, \delta_k = 1$), under the condition that the clocks oscillate at distinct frequencies (i.e. $\omega_i \neq \omega_j, \; \forall \;\; i \neq j$). Despite this vast simplification and theoretical observability, from a purely mathematical point of view, practical observability of these systems is ill-posed.

Inferences from this work for oscillatory distributed engineering systems (including future power grids and telecommunication systems) and oscillatory biological systems (including observation of neural activity in the brain) indicate that large scale observability is utopian. Instead concentrating on tracking dynamics within very localised subsystems of the network seems to be more achievable. This particularly has implications for tracking and predicting neural activity, for applications such as epileptic seizure prediction, where attempts to reconstruct underlying dynamics across large areas of the brain using relatively few electrodes are problematic.

ACKNOWLEDGEMENTS

This work is based on an ongoing collaborative effort between St. Vincent's Hospital, Melbourne and The School of Engineering, The University of Melbourne towards research in epilepsy. We want to acknowledge in particular Michelle Chong, Prof Mark Cook, Prof Anthony Burkitt, Dr Karen Fuller, Dr Dean Freestone, A/Prof David Grayden, Dr Levin Kuhlmann, Dr Alan Lai, Andre Peterson and Dr Andrea Varsavsky for many helpful discussions. In addition, many thanks to Prof Jonathan Manton for sifting out useful trigonometric identities from papers past.

REFERENCES

Bibak, K., Haghighi, M.S., et al. (2009). Some trigonometric identities involving fibonacci and lucas numbers. *Journal of Integer Sequences*, 12(2), 3.

Butler, D. (2007). Energy efficiency: Super savers: Meters to manage the future. *Nature*, 445(7128), 586–588.

Golub, G.H. and Van Loan, C.F. (2013). *Matrix computations*, volume 4. Johns Hopkins University Press.

Kailath, T. (ed.) (1980). *Linear systems*. Information & Science Series. Prentice-Hall.

Liu, Y.Y., Slotine, J.J., and Barabási, A.L. (2013). Observability of complex systems. *Proceedings of the National Academy of Sciences*, 110(7), 2460–2465.

Monticelli, A. and Wu, F.F. (1985). Network observability: identification of observable islands and measurement placement. *Power Apparatus and Systems, IEEE Transactions on*, 104(5), 1035–1041.

Niedermeyer, E. and Lopes Da Silva, F.H. (2005). *Electroencephalography: Basic Principles, Clinical Applications and Related Fields.* Lippincott Williams & Wilkins, 5th edition edition.

OSullivan-Greene, E., Kuhlmann, L., Varsavsky, A., Grayden, D.B., Burkitt, A.N., and Mareels, I.M.Y. (2011). *Seizure Prediction and Observability of EEG Sources.* In Epilepsy: The Intersection of Neurosciences, Biology, Mathematics, Engineering and Physics, Ed. Osorio, I. and Zaveri, H. and Frei, M. G. and Arthurs, S. CRC Press.

O'Sullivan-Greene, E., Mareels, I., Burkitt, A., and Kulhmann, L. (2009a). Observability issues in networked clocks with applications to epilepsy. In *Proceedings of the 48th IEEE Conference on Decision and Control (IEEE CDC)*, 3527–3532.

O'Sullivan-Greene, E., Mareels, I., Freestone, D., Kulhmann, L., and Burkitt, A. (2009b). A paradigm for epileptic seizure prediction using a coupled oscillator model of the brain. In *Proceedingsof the IEEE Engineering in Medicine and Biology Society (EMBC 2009)*, 6428–6431.

Prehofer, C. and Bettstetter, C. (2005). Self-organization in communication networks: principles and design paradigms. *Communications Magazine, IEEE*, 43(7), 78–85.

Rohden, M., Sorge, A., Timme, M., and Witthaut, D. (2012). Self-organized synchronization in decentralized power grids. *Physical Review Letters*, 109(6), 64101.

Strogatz, S.H. and Stewart, I. (1993). Coupled oscillators and biological synchronization. *Scientific American*, 269(6), 102–109.

Varsavsky, A., Mareels, I., and Cook, M. (2010). *Epileptic seizures and the EEG: measurement, models, detection and prediction.* CRC Press.

Wright, J.J., Kydd, R.R., and Lees, G.J. (1985). State-changes in the brain viewed as linear steady-states and non-linear transitions between steady-states. *Biological Cybernetics*, 53, 11–17.

Wu, F.F. and Monticelli, A. (1985). Network observability: theory. *Power Apparatus and Systems, IEEE Transactions on*, 105(5), 1042–1048.